Copyrights IEEE 2016

This is the accepted version of the paper entitled 'Cascade-like modular tracking controller for non-Standard N-Trailers' by M. M. Michałek (DOI:10.1109/TCST.2016.2557232) published in IEEE Transactions on Control Systems Technology, Vol. 25, No. 2, pp. 619-627, 2017, ©IEEE 2016

Cascade-like modular tracking controller for non-Standard N-Trailers

Maciej Marcin Michałek, *Senior Member, IEEE*, ©IEEE 2016

***Abstract*—A general trajectory tracking control solution is proposed for *truly* N-Trailer robots comprising a unicycle-like tractor and *arbitrary* number of passive trailers interconnected by sign-homogeneous non-zero hitching offsets. The solution permits either backward or forward motion strategy of a vehicle preserving location of a guidance point on the last trailer. The presented control law is modular and highly scalable with respect to a number of trailers thanks to employing a cascade-like control structure. Stability and robustness analysis of the closed-loop system provides sufficient conditions of asymptotic and practical tracking for a wide set of the so-called *segment-platooning* reference trajectories containing both constant-curvature and varying-curvature motion profiles. Efficiency of the controller and its robustness to parametric uncertainty have been illustrated by experimental results obtained for a three-trailer vehicle.**

***Index Terms*—trajectory tracking, cascade-like feedback control, N-Trailers, off-axle hitching**

I. Introduction

The N-Trailer vehicles (N-Trailers) play increasingly important role in contemporary ground transportation due to the economic and usage-flexibility reasons. One may predict that the recent trend for automation of guidance systems in commercial vehicles will find applications also in the domain of articulated vehicles which are especially difficult to control. Due to specific properties of N-Trailer kinematics (investigated e.g. in [1], [8], [10], [12], [13], [26]), feedback control design for these systems is generally non-trivial. Most control solutions proposed in the literature so far for *truly* N-Trailers (i.e. admitting *arbitrary* number of trailers) concern the time-non-critical tasks like the set-point stabilization and path following (see for instance [2]–[4], [9], [14], [15], [18], [21], [24], [27]), or address the control problems for the differentially flat so-called Standard N-Trailers (SNT) equipped solely with on-axle hitches, see [7], [19], [22], [24], [27].

In this work, the time-critical trajectory tracking problem is considered for truly N-Trailer robotic vehicles equipped with a unicycle-like tractor and a number of N trailers with non-steerable wheels interconnected in a chain by passive rotary joints. We focus on the N-Trailers equipped solely with off-axle hitches. Following classification proposed in [8], let us call the vehicles from this class the non-Standard-N-Trailers, or shortly: the nSNT vehicles. Essential difficulties with nSNT vehicles come from a combination of three features of their kinematics: joint-instability in backward motion, nonminimum-phaseness in forward motion with positive hitching offsets, and the lack of differential flatness if $N > 1$. Combination of these features makes nSNT kinematics an especially hard-to-control system. Numerous specialized tracking control laws have been devised for robots with strictly limited number of trailers – typically for $N \leq 2$. To the author's best knowledge, the only trajectory tracking control method elaborated for truly nSNT vehicles have been proposed in [5] employing a cascade-like concept (see also [28]), independently investigated in [17]. The cascade-like approach has revealed its big potential, however the authors of [5] restricted their considerations only to the special case of backward tracking of constant-curvature reference trajectories assuming omni-directional kinematics of a tractor and common positive lengths of all the hitching offsets equal to the trailer lengths. Local stability analysis provided in [5] was limited only to the case of $N = 1$ in the task of straight-line tracking. As a consequence, one may have a strong feeling that the promising control approach proposed in [5] has not been investigated deeply enough to reveal its real application potential.

The main objective and contribution of this work is extension, generalization, and formal analysis of the cascade-like trajectory tracking control system for truly nSNT robots based on the concept presented in [5]. A new generic description followed by stability and robustness analysis of a closed-loop system provide new insights into advantages and limitations of the proposed control approach. By removing restrictions imposed in [5], applicability of the controller is extended to nSNT kinematics admitting various lengths of trailers and hitching offsets. By introducing the so-called *segment-platooning* reference trajectories, sufficient conditions for asymptotic and practical tracking are provided for both constant-curvature and varying-curvature trajectories. This work builds upon the conference paper [16] and partly on the results presented in [15] for the path following task. In contrast to [15], the current paper concerns the trajectory tracking problem, and focuses on the modularity and robustness of the proposed control system.

II. N-Trailer kinematics and problem statement

A. Kinematics of N-Trailers

Configuration of the N-Trailer can be uniquely determined by the vector (see Fig. 1)

$$\boldsymbol{q} \triangleq [\beta_1 \ \ldots \ \beta_N \ \theta_N \ x_N \ y_N]^\top = \begin{bmatrix} \boldsymbol{\beta} \\ \boldsymbol{q}_N \end{bmatrix} \in \mathbb{T}^N \times \mathbb{R}^3, \quad (1)$$

where $\boldsymbol{\beta}$ and $\boldsymbol{q}_N$ denote, respectively, the joint-angle vector (the *shape* configuration) and the posture vector of the last trailer called the *guidance segment*. Posture $\boldsymbol{q}_N$ comprises the trailer-body orientation θ_N and position coordinates x_N, y_N of the *guidance point* P. Angular ω_0 and longitudinal v_0 velocities of a unicycle-like tractor are treated as components of the vehicle control input $\boldsymbol{u}_0 = [\omega_0 \ v_0]^\top$. N-Trailer kinematics is characterized by two kinds of parameters: trailer lengths $L_i > 0$ and hitching offsets $L_{hi} \in \mathbb{R}$, $i = 1, \ldots, N$. We adopt

The author is with the Chair of Control and Systems Engineering, Poznań University of Technology, Piotrowo 3a, 60-965 Poznań, Poland, e-mail: maciej.michalek@put.poznan.pl

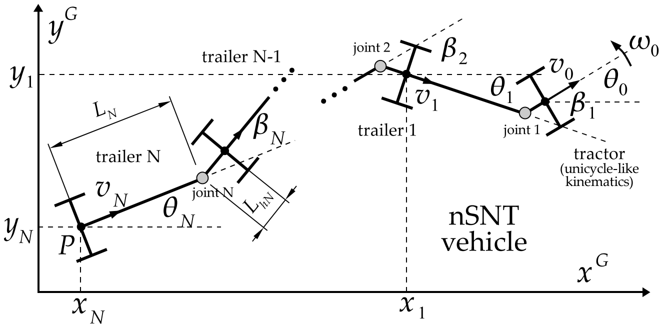

Fig. 1. Kinematic scheme of the nSNT robot in a global frame $\{x^G, y^G\}$.

the sign convention of hitching where $L_{hi} > 0$ if the ith joint is located *behind* the wheels-axle of the $(i-1)$st segment, while $L_{hi} < 0$ in the opposite case.

We will consider the N-Trailers satisfying assumptions:

A1. $\forall\, i \in \{1, \ldots, N\}\ L_{hi} \neq 0$,
A2. $L_{hi}L_{hj} > 0$ for all $i, j \in \{1, \ldots, N\}$,
A3. $\forall\, i \in \{1, \ldots, N\}\ |L_{hi}| < L_i$ if $L_{hi} < 0$.

A1 restricts our interest to the nSNT vehicles which are not differentially flat if $N > 1$. A2, dictated by stability conditions explained in Section IV, assumes the so-called *sign-homogeneous hitching* where all the hitching offsets have a common sign (all are positive or negative but can have different lengths). A3 comes from obvious mechanical reasons.

Key properties of nSNT kinematics utilized in the sequel result from treating the particular vehicle segments as unicycles (hereafter we will use the notation $\mathrm{s}\alpha \equiv \sin\alpha$, $\mathrm{c}\alpha \equiv \cos\alpha$)

$$\dot{\boldsymbol{q}}_i = \boldsymbol{G}(\boldsymbol{q}_i)\boldsymbol{u}_i, \quad \boldsymbol{G}(\boldsymbol{q}_i) \triangleq \begin{bmatrix} 1 & 0 & 0 \\ 0 & \mathrm{c}\theta_i & \mathrm{s}\theta_i \end{bmatrix}^\top, \tag{2}$$

where $\boldsymbol{q}_i = [\theta_i\ x_i\ y_i]^\top \in \mathbb{R}^3$ denotes a posture while $\boldsymbol{u}_i = [\omega_i\ v_i]^\top \in \mathbb{R}^2$ is a velocity vector of the ith segment. The direct and inverse transformations of velocities between any two neighboring segments result from equations (see e.g. [8]):

$$\boldsymbol{u}_i = \begin{bmatrix} -\frac{L_{hi}}{L_i}\mathrm{c}\beta_i & \frac{1}{L_i}\mathrm{s}\beta_i \\ L_{hi}\,\mathrm{s}\beta_i & \mathrm{c}\beta_i \end{bmatrix} \boldsymbol{u}_{i-1} = \boldsymbol{J}_i(\beta_i)\boldsymbol{u}_{i-1} \tag{3}$$

$$\boldsymbol{u}_{i-1} = \begin{bmatrix} \frac{-L_i}{L_{hi}}\mathrm{c}\beta_i & \frac{1}{L_{hi}}\mathrm{s}\beta_i \\ L_i\,\mathrm{s}\beta_i & \mathrm{c}\beta_i \end{bmatrix} \boldsymbol{u}_i = \boldsymbol{J}_i^{-1}(\beta_i)\boldsymbol{u}_i, \tag{4}$$

where the inverse matrix $\boldsymbol{J}_i^{-1}(\beta_i)$ is well determined for any β_i under assumption A1. Using (2) and (3), one can express kinematics of the N-Trailers as a drift-free system (see [8])

$$\underbrace{\begin{bmatrix} \dot{\boldsymbol{\beta}} \\ \dot{\boldsymbol{q}}_N \end{bmatrix}}_{\dot{\boldsymbol{q}}} = \underbrace{\begin{bmatrix} \boldsymbol{S}_\beta(\boldsymbol{\beta}) \\ \text{-----} \\ \boldsymbol{S}_N(\boldsymbol{\beta}, \boldsymbol{q}_N) \end{bmatrix}}_{\boldsymbol{S}(\boldsymbol{q})} \boldsymbol{u}_0 = \begin{bmatrix} \boldsymbol{c}^\top \boldsymbol{\Gamma}_1(\beta_1) \\ \boldsymbol{c}^\top \boldsymbol{\Gamma}_2(\beta_2)\boldsymbol{J}_1(\beta_1) \\ \vdots \\ \boldsymbol{c}^\top \boldsymbol{\Gamma}_N(\beta_N)\boldsymbol{J}_{N-1}^1(\boldsymbol{\beta}) \\ \text{---------} \\ \boldsymbol{c}^\top \boldsymbol{J}_N^1(\boldsymbol{\beta}) \\ \boldsymbol{d}^\top \boldsymbol{J}_N^1(\boldsymbol{\beta})\mathrm{c}\theta_N \\ \boldsymbol{d}^\top \boldsymbol{J}_N^1(\boldsymbol{\beta})\mathrm{s}\theta_N \end{bmatrix} \boldsymbol{u}_0, \tag{5}$$

where $\boldsymbol{\Gamma}_i(\beta_i) \triangleq \boldsymbol{I} - \boldsymbol{J}_i(\beta_i)$, $\boldsymbol{I} \in \mathbb{R}^{2\times 2}$ is the identity matrix, $\boldsymbol{J}_i^1(\boldsymbol{\beta}) \triangleq \boldsymbol{J}_i(\beta_i) \ldots \boldsymbol{J}_1(\beta_1)$, and $\boldsymbol{c}^\top \triangleq [1\ 0]$, $\boldsymbol{d}^\top \triangleq [0\ 1]$. Worth to note that system (5) under assumption A1 is not differentially flat for $N > 1$, that is, (5) cannot be transformed into the chained form in contrast to the Standard N-Trailers widely addressed in the literature [23], [24].

B. Control problem formulation

The motion task under consideration will rely on guiding the last trailer of a vehicle towards and then along a time-parametrized reference trajectory defined for the guidance segment, guaranteeing avoidance of the so-called jackknife effect in vehicle articulations[1].

Let us introduce the reference configuration trajectory

$$\boldsymbol{q}_r(t) \triangleq [\boldsymbol{\beta}_r^\top(t)\ \boldsymbol{q}_{Nr}^\top(t)]^\top \in \mathbb{T}^N \times \mathbb{R}^3 \tag{6}$$

which consists of the reference *shape* trajectory $\boldsymbol{\beta}_r(t)$ and the reference *guidance* trajectory $\boldsymbol{q}_{Nr}(t)$. Following the above formulation of a motion task, we complement kinematics (5) with output $\boldsymbol{y} \triangleq \boldsymbol{q}_N = [\boldsymbol{0}_{3\times N}\ \boldsymbol{I}_{3\times 3}]\boldsymbol{q}$, and define the corresponding reference output (guidance) trajectory

$$\boldsymbol{y}_r(t) \triangleq \boldsymbol{q}_{Nr}(t) = [\theta_{Nr}(t)\ x_{Nr}(t)\ y_{Nr}(t)]^\top \in \mathbb{R}^3. \tag{7}$$

Assume that (7) satisfies the following conditions:

C1. $\dot{\boldsymbol{q}}_{Nr}(t) = \boldsymbol{G}(\boldsymbol{q}_{Nr}(t))\boldsymbol{u}_{Nr}(t)$,
C2. $\forall\, t \geq 0\ \ \|\boldsymbol{u}_{Nr}(t)\| \neq 0$,
C3. $\forall\, t \geq 0\ \ \|\boldsymbol{u}_{Nr}(t)\| < \bar{u}_r < \infty$, $\|\dot{\boldsymbol{u}}_{Nr}(t)\| < \infty$,

where $\boldsymbol{u}_{Nr} = [\omega_{Nr}\ v_{Nr}]^\top \in \mathbb{R}^2$ is the reference (guiding) velocity along $\boldsymbol{q}_{Nr}(t)$. C1 imposes nonholonomic constraints on the reference trajectory making it *admissible* by satisfaction of unicycle-like kinematics (2). Condition C2 reflects a general *persistent excitation* condition for trajectory (7), whereas C3 assumes boundedness of reference velocities and accelerations along $\boldsymbol{q}_{Nr}(t)$.

Since nSNT kinematics is not differentially flat, it is generally not known (except some particular cases) how to explicitly find the reference shape trajectory $\boldsymbol{\beta}_r(t) = [\beta_{1r}(t) \ldots \beta_{Nr}(t)]^\top \in \mathbb{T}^N$ corresponding to reference guidance trajectory (7). One may compute the associated reference shape trajectory as a response of the exogenous system

$$\dot{\boldsymbol{\beta}}_r \overset{(5)}{=} \boldsymbol{S}_\beta(\boldsymbol{\beta}_r)\boldsymbol{u}_{0r} \overset{(4)}{=} \boldsymbol{S}_\beta(\boldsymbol{\beta}_r) \prod_{j=1}^{N} \boldsymbol{J}_j^{-1}(\beta_{jr})\boldsymbol{u}_{Nr} \tag{8}$$

with reference input $\boldsymbol{u}_{Nr}(t)$ which is known a priori or can be explicitly determined upon time-derivatives of (7). Thanks to the cascade-like control approach applied in the sequel, computations of reference signals (8) will not be required. It is sufficient to assume that a solution of (8) exists and is bounded.

Introducing the *shape-error* $\tilde{\boldsymbol{\beta}} = [\tilde{\beta}_1\ \ldots\ \tilde{\beta}_N]^\top$ and the *guidance-error* (output-error) $\boldsymbol{e}_N = [e_\theta\ e_x\ e_y]^\top$ as

$$\tilde{\boldsymbol{\beta}}(t) \triangleq \boldsymbol{\beta}_r(t) - \boldsymbol{\beta}(t), \qquad \boldsymbol{e}_N(t) \triangleq \boldsymbol{q}_{Nr}(t) - \boldsymbol{q}_N(t), \tag{9}$$

one formulates the trajectory-tracking control (TTC) problem.

Definition 1 (TTC Problem): For nSNT kinematics (5), satisfying assumptions A1-A3, find a bounded feedback control law $\boldsymbol{u}_0 = \boldsymbol{u}_0(\boldsymbol{q}_r(t), \boldsymbol{q}(t), \cdot)$ guaranteeing that $\tilde{\boldsymbol{\beta}}(t) \to \boldsymbol{0}$ and $\boldsymbol{e}_N(t) \to \boldsymbol{0}_{2\mu\pi}$ as $t \to \infty$, where $\boldsymbol{0}_{2\mu\pi} \triangleq [2\mu\pi\ 0\ 0]^\top$ is the *zero-set* defined for any $\mu \in \{0, \pm 1, \pm 2, \ldots\}$.

[1] In the literature, the jackknife effect is explained in various ways. For the purpose of our considerations, the jackknife will be understood hereafter as motion conditions where at least two neighboring vehicle segments have longitudinal velocities with opposed signs (when expressed in the particular segment-body frames), i.e., $v_{i-1}(t)v_i(t) < 0$.

Remark 1: Thanks to introducing the zero-set $\mathbf{0}_{2\mu\pi}$ one enables a wider class of control laws for a problem solution. As a consequence, by writing $\boldsymbol{e}_N = \mathbf{0}_{2\mu\pi}$ for $\mu = 0$ one understands a single point $\boldsymbol{e}_N = \mathbf{0}$, while the expression $\boldsymbol{e}_N = \mathbf{0}_{2\mu\pi}$ for $\mu = 0, \pm 1, \pm 2, \ldots$ means that $\boldsymbol{e}_N$ is equal to *any* point from the countable set of points $\{\mathbf{0}, \mathbf{0}_{\pm 2\pi}, \mathbf{0}_{\pm 4\pi}, \ldots\}$.

III. S-P REFERENCE TRAJECTORIES

Following the concept of the so-called segment-platooning reference paths, introduced for the first time in [15], let us define a subclass of *segment-platooning* (S-P) reference trajectories (6) which satisfy the *sufficient S-P condition*

$$\forall\, t \geq 0 \quad v_{i-1r}(t) \cdot v_{ir}(t) > 0, \qquad i = 1, \ldots, N, \tag{10}$$

where reference velocities $v_{ir}(t)$ can be found by recurrence application of (4): $v_{ir}(t) = [0\ 1] \cdot \prod_{j=i+1}^{N} \boldsymbol{J}_j^{-1}(\beta_{jr}(t)) \boldsymbol{u}_{Nr}(t)$. Inequality (10) determines a requirement, in which the reference longitudinal velocities of any two neighboring segments shall be non-zero and shall have the same signs along the reference trajectory defined by (7) and $\boldsymbol{\beta}_r(t)$.

The S-P trajectories do not force the so-called *jackknife effect* in vehicle articulations. To clarify this property let us investigate a special subset of reference configuration trajectories corresponding to the constant-curvature (rectilinear and circular) guidance trajectories $\boldsymbol{q}_{Nr}(t)$ characterized by the reference velocity $\boldsymbol{u}_{Nr} = [\omega_{Nr}\ v_{Nr}]^\top = \text{const}$. Let us write the ith row of the exogenous system (8) as follows

$$\dot{\beta}_{ir} = -\omega_{ir}[1 + (L_i/L_{hi})\text{c}\beta_{ir}] + v_{ir}(1/L_{hi})\text{s}\beta_{ir} \tag{11}$$
$$= \omega_{i-1r}[1 + (L_{hi}/L_i)\text{c}\beta_{ir}] - v_{i-1r}(1/L_i)\text{s}\beta_{ir}. \tag{12}$$

For the considered constant-curvature guidance trajectory the angular velocities $\omega_{ir} = \omega_{Nr} = \text{const}$ and longitudinal velocities $v_{ir} = \text{const}$ for all $i = 0, \ldots, N$. By inspection of (12), it can be checked that the steady reference angle

$$\bar{\beta}_{ir} = \text{Atan2}\left(\text{s}\bar{\beta}_{ir}, \text{c}\bar{\beta}_{ir}\right) \in [-\pi, \pi) \tag{13}$$
$$\text{s}\bar{\beta}_{ir} = \omega_{Nr}(L_i v_{i-1r} + L_{hi} v_{ir})/(v_{i-1r}^2 + \omega_{Nr}^2 L_{hi}^2) \tag{14}$$
$$\text{c}\bar{\beta}_{ir} = (v_{ir} v_{i-1r} - \omega_{Nr}^2 L_i L_{hi})/(v_{i-1r}^2 + \omega_{Nr}^2 L_{hi}^2) \tag{15}$$

determines possible equilibria of joint-angle reference dynamics. Linearization of (11) around the working point $(\bar{\beta}_{ir}, \omega_{Nr}, v_{ir})$ gives the approximated dynamics

$$\dot{\beta}_{ir} \approx \frac{v_{i-1r}}{L_{hi}} \cdot \frac{v_{ir}^2 + \omega_{Nr}^2 L_i^2}{v_{i-1r}^2 + \omega_{Nr}^2 L_{hi}^2} (\beta_{ir} - \bar{\beta}_{ir}). \tag{16}$$

Upon (13)-(15), one may observe that

$$\bar{\beta}_{ir} \in \left(-\frac{\pi}{2}; \frac{\pi}{2}\right) \quad \Leftrightarrow \quad v_{ir} v_{i-1r} > \omega_{Nr}^2 L_i L_{hi}, \tag{17}$$

while $\bar{\beta}_{ir} \in [-\pi; -\frac{\pi}{2}] \cup [\frac{\pi}{2}; \pi)$ otherwise. One may say that inequality in (17) represents a (conservative) *safety condition* preventing the jackknife effect in the ith articulation of a reference vehicle. For rectilinear guidance trajectories $\omega_{Nr} \equiv 0$, and (17) reduces to condition (10). For circular guidance trajectories, (10) is a necessary (if $L_{hi} > 0$) or sufficient (if $L_{hi} < 0$) condition for satisfaction of inequality in (17). Therefore, one may treat (10) as a less conservative condition for the jackknife effect avoidance in the sense, that it is still possible to meet (10) for circular guidance trajectories even if $|\bar{\beta}_{ir}| \geq \frac{\pi}{2}$, which may be acceptable in some applications.

The second conclusion comes from equation (16), upon which one can find that (local) asymptotic stability of equilibrium $\bar{\beta}_{ir}$ requires $\frac{v_{i-1r}}{L_{hi}} < 0$. It means that the *necessary S-P condition* can be formulated as follows

$$\text{sgn}(v_{i-1r}) = -\text{sgn}(L_{hi}) \quad \forall\, i = 1, \ldots, N, \tag{18}$$

where $\text{sgn}(\cdot)$ is a sign-function. Although the necessary S-P condition (18) has been deduced for the constant-curvature guidance trajectories, it turns out to be valid also for more general trajectories as will be shown in the next sections. By combining (18) with (10) one may write the *S-P condition*

$$\text{sgn}(v_{i-1r}) = \text{sgn}(v_{ir}) = -\text{sgn}(L_{hi}) \quad \forall\, i = 1, \ldots, N \tag{19}$$

imposing additional restriction on the reference guidance trajectory, which permits the backward reference motion only if $L_{hi} > 0$ or the forward reference motion only if $L_{hi} < 0$ for all $i = 1, \ldots, N$ (condition (19) requires satisfaction of assumption A2). Relaxation of this limitation is possible to some extent (see Section VI) thanks to robustness property of the closed-loop system addressed in Section V.

IV. MODULAR TRACKING CONTROLLER

The control concept is based on the inverse relation (4), which applied recursively for $i = 1, \ldots, N$ allows us to write $\boldsymbol{u}_0 = \prod_{j=1}^{N} \boldsymbol{J}_j^{-1}(\beta_j) \boldsymbol{u}_N$. This purely algebraic equation reflects how velocity $\boldsymbol{u}_N$ of the guidance segment can be forced by tractor input $\boldsymbol{u}_0$ in the nSNT kinematics. Therefore, let us propose the following cascade-like control law

$$\boldsymbol{u}_0(\boldsymbol{\beta}, \boldsymbol{\Phi}) = \begin{bmatrix} \omega_0(\boldsymbol{\beta}, \boldsymbol{\Phi}) \\ v_0(\boldsymbol{\beta}, \boldsymbol{\Phi}) \end{bmatrix} \triangleq \prod_{j=1}^{N} \boldsymbol{J}_j^{-1}(\beta_j) \boldsymbol{\Phi}(\boldsymbol{e}_N, t), \tag{20}$$

where $\boldsymbol{\Phi}(\boldsymbol{e}_N, t) = [\Phi_\omega(\boldsymbol{e}_N, t)\ \Phi_v(\boldsymbol{e}_N, t)]^\top : \mathbb{R}^3 \times \mathbb{R}_{\geq 0} \to \mathbb{R}^2$ is some feedback control function which depends on the guidance-error defined in (9). To keep generality of considerations, we will not specify here any particular form of $\boldsymbol{\Phi}(\boldsymbol{e}_N, t)$; assume only that it has three key properties:

P1. $\forall\, t \geq 0\ \ \|\boldsymbol{\Phi}(\boldsymbol{e}_N(t), t)\| \leq \bar{\phi} < \infty$,
P2. $\forall\, t \geq 0\ \boldsymbol{\Phi}(\mathbf{0}_{2\mu\pi}, t) = \boldsymbol{u}_{Nr}(t)$,
P3. $\forall\, t \geq 0\ \ \boldsymbol{u}_N(t) = \boldsymbol{\Phi}(\boldsymbol{e}_N(t), t)$ makes $\boldsymbol{e}_N = \mathbf{0}_{2\mu\pi}$ the uniformly in time asymptotically stable equilibrium (equilibria) of guidance-error dynamics (cf. (9), (2), C1)

$$\dot{\boldsymbol{e}}_N = \boldsymbol{\zeta}(\boldsymbol{e}_N, t) \tag{21}$$

where $\boldsymbol{\zeta}(\boldsymbol{e}_N, t) = \boldsymbol{G}(\boldsymbol{q}_{Nr})\boldsymbol{u}_{Nr} - \boldsymbol{G}(\boldsymbol{q}_{Nr} - \boldsymbol{e}_N)\boldsymbol{\Phi}(\boldsymbol{e}_N, t)$.

Property P1 indicates boundedness of control function $\boldsymbol{\Phi}$. P2 guarantees that $\boldsymbol{\Phi}$ is well determined along the reference guidance trajectory (i.e. for $\boldsymbol{e}_N(t) \equiv \mathbf{0}_{2\mu\pi}$) and corresponds there to the reference guiding velocity. P3 means that direct application of $\boldsymbol{\Phi}(\boldsymbol{e}_N, t)$ into kinematics of the guidance segment (by forcing $\boldsymbol{u}_N(t) = \boldsymbol{\Phi}(\boldsymbol{e}_N, t)$ in (2) for $i = N$) guarantees asymptotic tracking of the reference output trajectory (7) in the sense of Definition 1. Thus, $\boldsymbol{\Phi}(\boldsymbol{e}_N, t)$ represents one of the tracking control laws presented in the literature for unicycle kinematics (see e.g. [6], [20]). Properties of function $\boldsymbol{\Phi}$ will

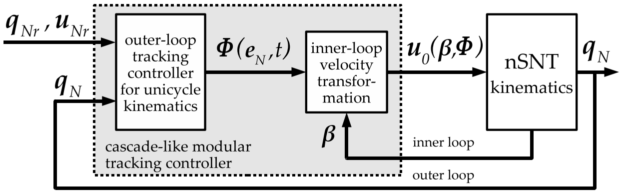

Fig. 2. Block scheme of the proposed cascade-like control system.

determine both the value(s) of μ and the basin(s) of attraction for point(s) $\boldsymbol{e}_N = \boldsymbol{0}_{2\mu\pi}$.

Note that (20) defines the cascade-like interconnection of the outer-loop tracking controller $\boldsymbol{\Phi}(\boldsymbol{e}_N, t)$, and the inner-loop velocity transformation in the form of product $\boldsymbol{J}_1^{-1}(\beta_1)\ldots\boldsymbol{J}_N^{-1}(\beta_N)$ evaluated at the current shape configuration of a vehicle. A general scheme explaining the considered control structure is shown in Fig. 2. Worth emphasizing modularity and scalability of the control structure which, respectively, result from applicability of various functions $\boldsymbol{\Phi}(\boldsymbol{e}_N, t)$ in the outer-loop, and from the simple inner-loop velocity transformation where a number of trailers affects only a number of matrices used in the product.

Theorem 1: Cascade-like control law (20), with outer-loop control function $\boldsymbol{\Phi}(\boldsymbol{e}_N, t)$ possessing properties P1-P3, solves the TTC Problem locally in a neighborhood of $(\tilde{\boldsymbol{\beta}}, \boldsymbol{e}_N) = (\boldsymbol{0}, \boldsymbol{0}_{2\mu\pi})$ for the S-P reference trajectories $\boldsymbol{q}_r(t)$ satisfying C1-C3 together with (19) when:

(I) $\dot{\boldsymbol{u}}_{Nr}(t) \equiv \boldsymbol{0} \ \Rightarrow\ \boldsymbol{u}_{Nr} = \text{const}$, or

(II) $\dot{\boldsymbol{u}}_{Nr}(t) \not\equiv \boldsymbol{0}$ if $\forall\, t \geq 0\ \ \|\boldsymbol{u}_{Nr}(t)\| \leq \delta_1$ and $\|\dot{\boldsymbol{u}}_{Nr}(t)\| \leq \delta_2$ for sufficiently small constants $\delta_1, \delta_2 > 0$.

Proof: Since this part is analogous to the analysis presented in [16] (and partly in [15]), we will recall here only main reasoning stages helpful for subsequent considerations.

First note that boundedness of control vector (20) directly results from property P1 and from boundedness of $\|\boldsymbol{J}_j^{-1}(\beta_j)\|$ under assumption A1. Second, upon (3) and (20) one can write $\boldsymbol{u}_N = \prod_{j=N}^{1} \boldsymbol{J}_j(\beta_j) \prod_{j=1}^{N} \boldsymbol{J}_j^{-1}(\beta_j)\boldsymbol{\Phi}(\boldsymbol{e}_N, t) = \boldsymbol{\Phi}(\boldsymbol{e}_N, t)$. Thus, application of (20) makes the guidance segment move in a way as it would be directly controlled by function $\boldsymbol{\Phi}(\boldsymbol{e}_N, t)$. According to P3, one concludes $\forall\, t \geq 0\ \ \|\boldsymbol{e}_N(t)\| < \infty$ and $\boldsymbol{e}_N(t \to T) \to \boldsymbol{0}_{2\mu\pi}$ for $T \in (0, \infty)$ and any $\mu \in \{0, \pm1, \pm2, \ldots\}$. The particular value(s) of μ and the basin(s) of attraction of point(s) $\boldsymbol{0}_{2\mu\pi}$ depend on properties of the particular function $\boldsymbol{\Phi}(\boldsymbol{e}_N, t)$ applied in the outer loop.

Next, we shall investigate behavior of the shape-error dynamics. Define the outer-loop control difference

$$\tilde{\boldsymbol{\Phi}}(t) \triangleq \boldsymbol{u}_{Nr}(t) - \boldsymbol{\Phi}(\boldsymbol{e}_N(t), t). \tag{22}$$

By taking a time-derivative of $\tilde{\boldsymbol{\beta}}$ defined in (9) and utilizing (5), (8), and (22) one can write the shape-error dynamics

$$\dot{\tilde{\boldsymbol{\beta}}} = \dot{\boldsymbol{\beta}}_r - \boldsymbol{S}_\beta(\boldsymbol{\beta}_r - \tilde{\boldsymbol{\beta}}) \prod_{j=1}^{N} \boldsymbol{J}_j^{-1}(\beta_{jr} - \tilde{\beta}_j)(\boldsymbol{u}_{Nr} - \tilde{\boldsymbol{\Phi}}) \tag{23}$$

which possess the equilibrium at $(\tilde{\boldsymbol{\beta}} = \boldsymbol{0}, \tilde{\boldsymbol{\Phi}} = \boldsymbol{0})$. Closer investigation of (23) reveals its upper-triangular form where the ith row, $i = 1, \ldots, N$, can be represented by equation

$$\dot{\tilde{\beta}}_i = f_i(\tilde{\boldsymbol{\beta}}_i^N, \boldsymbol{\beta}_r, \boldsymbol{u}_{Nr}) + g_i(\tilde{\boldsymbol{\beta}}_i^N, \boldsymbol{\beta}_r, \tilde{\boldsymbol{\Phi}}) \tag{24}$$

where $\tilde{\boldsymbol{\beta}}_i^N \triangleq [\tilde{\beta}_i\ \tilde{\beta}_{i+1}\ \ldots\ \tilde{\beta}_N]^\top$. Linearization of (23) around the equilibrium yields the approximate shape-error dynamics

$$\dot{\tilde{\boldsymbol{\beta}}} = \boldsymbol{A}(\boldsymbol{\beta}_r, \boldsymbol{u}_{Nr})\tilde{\boldsymbol{\beta}} + \boldsymbol{B}(\boldsymbol{\beta}_r)\tilde{\boldsymbol{\Phi}}, \tag{25}$$

where $\boldsymbol{A}(\boldsymbol{\beta}_r, \boldsymbol{u}_{Nr})$ is upper-triangular with diagonal elements

$$a_{ii} = v_{i-1r}/L_{hi} \quad \text{for} \quad i = 1, \ldots, N. \tag{26}$$

System (25) can be understood as the (approximate) *inner dynamics* of the closed-loop system. Treating $\tilde{\boldsymbol{\Phi}}$ in (25) as a perturbing input vanishing in time, one may analyze dynamics (25) under perfect output-tracking conditions where $\boldsymbol{e}_N = \boldsymbol{0}_{2\mu\pi}$ implying $\tilde{\boldsymbol{\Phi}}(t) \equiv \boldsymbol{0}$ (see (22) and P2). Now,

$$\dot{\tilde{\boldsymbol{\beta}}} = \boldsymbol{A}(\boldsymbol{\beta}_r, \boldsymbol{u}_{Nr})\,\tilde{\boldsymbol{\beta}} \tag{27}$$

approximates the *zero-dynamics* of the closed-loop system. Eigenvalues of matrix $\boldsymbol{A}$ correspond to (26) which become negative under the S-P condition determined by (19):

$$a_{ii} = \frac{\text{sgn}(v_{i-1r})\,|v_{i-1r}|}{\text{sgn}(L_{hi})\,|L_{hi}|} \overset{(18)}{=} \frac{-|v_{i-1r}|}{|L_{hi}|} \leq -\alpha, \tag{28}$$

where $\alpha = \min_{i\in\{1,\ldots,N\}} \left\{\inf_{t\geq0} \left|\frac{v_{i-1r}(t)}{L_{hi}}\right|\right\} > 0$ is strictly positive for the S-P reference trajectories thanks to the acute inequality in (10). We must separately consider two possible cases: (I) when $\boldsymbol{u}_{Nr} = \text{const}$, and (II) when $\boldsymbol{u}_{Nr} = \boldsymbol{u}_{Nr}(t)$. In case (I), $\boldsymbol{\beta}_r = \text{const}$, thus $\boldsymbol{A}(\boldsymbol{\beta}_r, \boldsymbol{u}_{Nr})$ becomes time-invariant and local uniform exponential stability of $\tilde{\boldsymbol{\beta}} = \boldsymbol{0}$ results directly from (28). In case (II), one has to further investigate properties of matrix $\boldsymbol{A}(\boldsymbol{\beta}_r(t), \boldsymbol{u}_{Nr}(t)) = \boldsymbol{A}(t)$ and its time-derivative $\dot{\boldsymbol{A}}(t)$. One can observe, by taking into account the forms of components (26) under assumption A1, that $\|\boldsymbol{A}(t)\| < \bar{A} < \infty$ for all $t \geq 0$. Furthermore, it can be shown (using (26), A1, C3, (8), and (5)) that a spectral norm of $\dot{\boldsymbol{A}}$ is bounded, i.e., $\forall\, t \geq 0\ \|\dot{\boldsymbol{A}}(t)\| \leq N\,(\zeta_1\delta_1 + \zeta_2\delta_2)$, where ζ_1, ζ_2 are some finite positive constants, see [16]. Ensuring that δ_1 and δ_2 are sufficiently small the right-hand side of the latter inequality can be made small enough to satisfy the sufficient condition for (uniform in time) asymptotic stability of the LTV system (27), see [25], [29]. ∎

Remark 2: Matrices $\boldsymbol{J}_j^{-1}(\beta_j)$ in (20) make the closed-loop system sensitive to a measurement noise corrupting the outer loop if hitching offsets are very small (cf. [17]). Sensitivity can be attenuated by using artificially increased values of $|L_{hj}|$ in computations of $\boldsymbol{J}_j^{-1}(\beta_j)$ at the expense of only ultimate boundedness of tracking errors (see Sections V and VI).

V. Robustness to parametric uncertainty

We are going to investigate stability robustness of the closed-loop system to parametric uncertainty of the vehicle model. To this aim, let us introduce the approximated matrix

$$\hat{\boldsymbol{J}}_i^{-1}(\beta_i) \triangleq \begin{bmatrix} -\frac{\hat{L}_i}{\hat{L}_{hi}}\text{c}\beta_i & \frac{1}{\hat{L}_{hi}}\text{s}\beta_i \\ \hat{L}_i\text{s}\beta_i & \text{c}\beta_i \end{bmatrix}, \qquad \begin{matrix} \hat{L}_i \triangleq \rho_i L_i \\ \hat{L}_{hi} \triangleq \rho_{hi} L_{hi} \end{matrix}, \tag{29}$$

where $\rho_i > 0$ and $\rho_{hi} \neq 0$ determine uncertainty of model parameters $\hat{L}_i$ and $\hat{L}_{hi}$ with respect to the nominal (true) values. By direct computations it can be checked that

$$\hat{\boldsymbol{J}}_i^{-1}(\beta_i) = \boldsymbol{J}_i^{-1}(\beta_i) + \boldsymbol{\Delta}_i(\beta_i, \tilde{L}_{hi}, \tilde{L}_i), \tag{30}$$

where $\tilde{L}_i \triangleq \hat{L}_i - L_i$ and $\tilde{L}_{hi} \triangleq \hat{L}_{hi} - L_{hi}$ are the parameter errors, while the perturbing matrix

$$\boldsymbol{\Delta}_i = \begin{bmatrix} \frac{1}{\rho_{hi} L_{hi}^2}\left(L_i \tilde{L}_{hi} - L_{hi}\tilde{L}_i\right)\mathrm{c}\beta_i & \frac{-1}{\rho_{hi} L_{hi}^2}\tilde{L}_{hi}\mathrm{s}\beta_i \\ \tilde{L}_i \mathrm{s}\beta_i & 0 \end{bmatrix} \quad (31)$$

has the norm bounded by a non-negative function, that is,

$$\|\boldsymbol{\Delta}_i\| \leq \frac{\nu_i|\tilde{L}_{hi}| + |\tilde{L}_i|}{|\tilde{L}_{hi} + L_{hi}|} + |\tilde{L}_i| =: D_i(\tilde{L}_{hi}, \tilde{L}_i), \quad (32)$$

where $\nu_i = \frac{1+L_i}{|L_{hi}|} > 0$ is finite (upon A1), while $D_i : \mathbb{R}\times\mathbb{R} \to \mathbb{R}_{\geq 0}$ is continuous in a neighborhood of zero and $D_i(0,0) = 0$.

Stability robustness will be investigated assuming that approximated matrices (29) are used in the controller (20) for some $\rho_i \neq 1$ and $\rho_{hi} \neq 1$. For conciseness, we will also use the vectorial terms: $\tilde{\boldsymbol{L}}_h \triangleq [\tilde{L}_{h1} \ldots \tilde{L}_{hN}]^\top$, $\tilde{\boldsymbol{L}} \triangleq [\tilde{L}_1 \ldots \tilde{L}_N]^\top$.

A. Stability robustness analysis for guidance-error dynamics

Under conditions of uncertainty, we need to replace nominal equation (20) with its approximated counterpart $\boldsymbol{u}_0(\boldsymbol{\beta}, \boldsymbol{\Phi}) \triangleq \prod_{j=1}^{N} \hat{\boldsymbol{J}}_j^{-1}(\beta_j)\boldsymbol{\Phi}(\boldsymbol{e}_N, t)$ which allows us to write

$$\begin{aligned} \boldsymbol{u}_N &\overset{(4)}{=} \prod_{j=N}^{1}\boldsymbol{J}_j(\beta_j)\boldsymbol{u}_0 = \prod_{j=N}^{1}\boldsymbol{J}_j(\beta_j)\prod_{j=1}^{N}\hat{\boldsymbol{J}}_j^{-1}(\beta_j)\boldsymbol{\Phi}(\boldsymbol{e}_N, t) \\ &\overset{(30)}{=} \prod_{j=N}^{1}\boldsymbol{J}_j(\beta_j)\prod_{j=1}^{N}[\boldsymbol{J}_j^{-1}(\beta_j) + \boldsymbol{\Delta}_j(\beta_j, \tilde{L}_{hi}, \tilde{L}_i)]\boldsymbol{\Phi}(\boldsymbol{e}_N, t) \\ &= \boldsymbol{\Phi}(\boldsymbol{e}_N, t) + \boldsymbol{H}(\boldsymbol{\beta}, \tilde{\boldsymbol{L}}_h, \tilde{\boldsymbol{L}})\boldsymbol{\Phi}(\boldsymbol{e}_N, t), \end{aligned} \quad (33)$$

where matrix $\boldsymbol{H}(\boldsymbol{\beta}, \tilde{\boldsymbol{L}}_h, \tilde{\boldsymbol{L}})$ results from the appropriate sum of products of matrices $\boldsymbol{J}_i$, $\boldsymbol{J}_i^{-1}$, and $\boldsymbol{\Delta}_i$, for $i \in \{1, \ldots, N\}$, and $\boldsymbol{H}(\boldsymbol{\beta}, \boldsymbol{0}, \boldsymbol{0}) = \boldsymbol{0}_{2\times 2}$ for all $\boldsymbol{\beta}$. Upon equation (33) one can alternatively write

$$\boldsymbol{H}(\boldsymbol{\beta}, \tilde{\boldsymbol{L}}_h, \tilde{\boldsymbol{L}}) = \prod_{j=N}^{1}\boldsymbol{J}_j(\beta_j)\prod_{j=1}^{N}\hat{\boldsymbol{J}}_j^{-1}(\beta_j) - \boldsymbol{I}, \quad (34)$$

which can be further reformulated as (omitting the arguments)

$$\begin{aligned} \boldsymbol{H} &= \prod_{j=N}^{1}\boldsymbol{J}_j\left[\prod_{j=1}^{N}(\boldsymbol{J}_j^{-1} + \boldsymbol{\Delta}_j) - \prod_{j=1}^{N}\boldsymbol{J}_j^{-1}\right] \\ &= \prod_{j=N}^{1}\boldsymbol{J}_j\left[\sum_{i=1}^{2^N-2}\boldsymbol{C}_i(\boldsymbol{J}_{\mathcal{Z}_k^i}^{-1}, \boldsymbol{\Delta}_{\mathcal{Z}_l^i}) + \prod_{j=1}^{N}\boldsymbol{\Delta}_j\right], \end{aligned} \quad (35)$$

where $\sum_{i=1}^{2^N-2}\boldsymbol{C}_i(\boldsymbol{J}_{\mathcal{Z}_k^i}^{-1}, \boldsymbol{\Delta}_{\mathcal{Z}_l^i})$ represents the sum of all the *mixed* products $\boldsymbol{C}_i$ of N matrices $\boldsymbol{J}_{\mathcal{Z}_k^i}^{-1}$ and $\boldsymbol{\Delta}_{\mathcal{Z}_l^i}$, with indexes from sets $\mathcal{Z}_k^i$ and $\mathcal{Z}_l^i$, respectively, which appear in the product $\prod_{j=1}^{N}(\boldsymbol{J}_j^{-1} + \boldsymbol{\Delta}_j)$. Assuming now that for all $\beta_j \in \mathbb{T}$ hold $\|\boldsymbol{J}_j(\beta_j)\| \leq M_j$ and $\left\|\boldsymbol{J}_j^{-1}(\beta_j)\right\| \leq m_j$ for some finite constants $M_j, m_j > 0$ (see definitions (3)-(4)), and by recalling (32), one can assess upon (35) what follows

$$\begin{aligned} \|\boldsymbol{H}\| &\leq \prod_{j=N}^{1}M_j\left[\sum_{i=1}^{2^N-2}\left\|\boldsymbol{C}_i(\boldsymbol{J}_{\mathcal{Z}_k^i}^{-1}, \boldsymbol{\Delta}_{\mathcal{Z}_l^i})\right\| + \prod_{j=1}^{N}D_j\right] \\ &\leq \bar{M}\left[\sum_{i=1}^{2^N-2}\prod_{\mathcal{Z}_{k,l}^i}[m_k \circ D_l]_i^N + D\right] =: \bar{H}(\tilde{\boldsymbol{L}}_h, \tilde{\boldsymbol{L}}) \end{aligned} \quad (36)$$

where $\bar{M} = \prod_{j=N}^{1}M_j$, $D = \prod_{j=1}^{N}D_j(\tilde{L}_{hj}, \tilde{L}_j)$, $[m_k \circ D_l]_i^N$ denotes the ith mixed product of N terms comprising constants m_k and functions $D_l(\tilde{L}_{hl}, \tilde{L}_l)$ with indexes from sets $\mathcal{Z}_k^i$ and $\mathcal{Z}_l^i$, respectively. Since $D_j(\tilde{L}_{hj}, \tilde{L}_j)$ and $D_l(\tilde{L}_{hl}, \tilde{L}_l)$ are of the form (32), the bound $\bar{H} : \mathbb{R}^N \times \mathbb{R}^N \to \mathbb{R}_{\geq 0}$ is a function continuous near zero, and $\bar{H}(\tilde{\boldsymbol{L}}_h \to \boldsymbol{0}, \tilde{\boldsymbol{L}} \to \boldsymbol{0}) \to 0$.

Using (33), the guidance-error dynamics (21) takes the form

$$\dot{\boldsymbol{e}}_N = \boldsymbol{\zeta}(\boldsymbol{e}_N, t) + \boldsymbol{d}(\boldsymbol{e}_N, t), \quad (37)$$

where $\boldsymbol{d}(\boldsymbol{e}_N, t) = -\boldsymbol{G}(\boldsymbol{q}_{Nr} - \boldsymbol{e}_N)\boldsymbol{H}(\boldsymbol{\beta}, \tilde{\boldsymbol{L}}_h, \tilde{\boldsymbol{L}})\boldsymbol{\Phi}(\boldsymbol{e}_N, t)$ is the perturbation term of nominal dynamics (21). Since in general $\boldsymbol{d}(\boldsymbol{0}_{2\mu\pi}, t) \not\equiv \boldsymbol{0}$, thus $\boldsymbol{e}_N = \boldsymbol{0}_{2\mu\pi}$ cannot be treated as an equilibrium (equilibria) of (37). Although, we can show the ultimate boundedness of error $\boldsymbol{e}_N(t)$. Recalling property P1, the upper bound (36), and the form of matrix $\boldsymbol{G}(\cdot)$ (see (2)) we get

$$\forall\, t \geq 0 \;\; \|\boldsymbol{d}(\boldsymbol{e}_N(t), t)\| \leq \bar{G}\bar{\phi}\bar{H}(\tilde{\boldsymbol{L}}_h, \tilde{\boldsymbol{L}}) =: \bar{d}(\tilde{\boldsymbol{L}}_h, \tilde{\boldsymbol{L}}), \quad (38)$$

where $\bar{G}$ is the upper bound of $\|\boldsymbol{G}(\cdot)\|$, while $\bar{d} : \mathbb{R}^N \times \mathbb{R}^N \to \mathbb{R}_{\geq 0}$ is a function continuous near zero, and $\bar{d}(\tilde{\boldsymbol{L}}_h \to \boldsymbol{0}, \tilde{\boldsymbol{L}} \to \boldsymbol{0}) \to 0$. Since $\boldsymbol{e}_N = \boldsymbol{0}_{2\mu\pi}$ constitutes the (uniformly in time) asymptotically stable equilibrium (equilibria) of nominal dynamics (21), one can use Lemma 9.3 formulated in [11] to state what follows.

Corollary 1: For sufficiently small $\bar{d}(\tilde{\boldsymbol{L}}_h, \tilde{\boldsymbol{L}})$, corresponding to sufficiently small $\left|\tilde{L}_{hi}\right|$ and $\left|\tilde{L}_i\right|$ for $i = 1, \ldots, N$, and for sufficiently small $\|\boldsymbol{e}_N(0)\|$ the solution of perturbed dynamics (37) is ultimately bounded (uniformly in time) satisfying

$$\|\boldsymbol{e}_N(t)\| \leq \xi_e(\|\boldsymbol{e}_N(0)\|, t) \qquad \text{for } t \in [0, T_e), \quad (39)$$

$$\|\boldsymbol{e}_N(t)\| \leq \kappa_e(\bar{d}(\tilde{\boldsymbol{L}}_h, \tilde{\boldsymbol{L}})) \qquad \text{for } t \in [T_e, \infty), \quad (40)$$

where $T_e > 0$ denotes a finite time instant, ξ_e is a function of class $\mathcal{KL}$, while κ_e is a function of class $\mathcal{K}$.

Remark 3: A maximal admissible magnitude of $\bar{d}(\tilde{\boldsymbol{L}}_h, \tilde{\boldsymbol{L}})$ and $\|\boldsymbol{e}_N(0)\|$ guaranteeing boundedness (39)-(40) essentially depends on the properties of function $\boldsymbol{\Phi}(\boldsymbol{e}_N, t)$ applied in the outer loop, see [11] pp. 347-350. In a special case, if $\boldsymbol{\Phi}(\boldsymbol{e}_N, t)$ nominally (i.e., for $\tilde{\boldsymbol{L}}_h = \boldsymbol{0}, \tilde{\boldsymbol{L}} = \boldsymbol{0}$) ensures global exponential stability of $\boldsymbol{e}_N = \boldsymbol{0}$, the magnitude of $\bar{d}(\tilde{\boldsymbol{L}}_h, \tilde{\boldsymbol{L}})$ can be arbitrarily large.

B. Stability robustness analysis for shape-error dynamics

For the case of parametric uncertainty, let us define the outer-loop control difference as follows

$$\begin{aligned} \tilde{\boldsymbol{u}}_N(t) &\triangleq \boldsymbol{u}_{Nr}(t) - \boldsymbol{u}_N(t) \\ &\overset{(33)}{=} \boldsymbol{u}_{Nr}(t) - [\boldsymbol{I} + \boldsymbol{H}]\boldsymbol{\Phi}(t) \overset{(22)}{=} \tilde{\boldsymbol{\Phi}}(t) - \boldsymbol{H}\boldsymbol{\Phi}(t), \end{aligned} \quad (41)$$

which reduces to the nominal outer-loop control difference (22) in the case of no uncertainty (i.e., for $\boldsymbol{H} = \boldsymbol{0}$). In the uncertainty conditions, one shall rewrite (23) in the form

$$\dot{\tilde{\boldsymbol{\beta}}} = \dot{\boldsymbol{\beta}}_r - \boldsymbol{S}_\beta(\boldsymbol{\beta})\prod_{j=1}^{N}\hat{\boldsymbol{J}}_j^{-1}(\beta_j)(\boldsymbol{u}_{Nr} - \tilde{\boldsymbol{\Phi}} + \boldsymbol{H}\boldsymbol{\Phi}), \quad (42)$$

where $\dot{\boldsymbol{\beta}}_r \overset{(8)}{=} \boldsymbol{S}_\beta(\boldsymbol{\beta}_r)\prod_{j=1}^{N}\boldsymbol{J}_j^{-1}(\beta_{jr})\boldsymbol{u}_{Nr}$, while $\hat{\boldsymbol{J}}_j^{-1}(\beta_j)$ results from (29). Upon the form of $\boldsymbol{S}_\beta(\boldsymbol{\beta})$ defined in (5), the ith row of (42) can be written as (omitting the arguments):

$$\begin{aligned}\dot{\tilde{\beta}}_i &= \dot{\beta}_{ir} - \boldsymbol{c}^\top[\boldsymbol{I}-\boldsymbol{J}_i]\prod_{j=i-1}^{1}\boldsymbol{J}_j\prod_{j=1}^{N}\hat{\boldsymbol{J}}_j^{-1}\cdot(\boldsymbol{u}_{Nr}-\tilde{\boldsymbol{\Phi}}+\boldsymbol{H}\boldsymbol{\Phi})\\ &= \dot{\beta}_{ir} - \boldsymbol{w}_i^\top\prod_{j=i}^{N}\boldsymbol{J}_j^{-1}\prod_{j=N}^{1}\boldsymbol{J}_j\prod_{j=1}^{N}\hat{\boldsymbol{J}}_j^{-1}\cdot(\boldsymbol{u}_{Nr}-\tilde{\boldsymbol{\Phi}}+\boldsymbol{H}\boldsymbol{\Phi})\\ &\overset{(34)}{=} \dot{\beta}_{ir} - \boldsymbol{w}_i^\top\prod_{j=i}^{N}\boldsymbol{J}_j^{-1}[\boldsymbol{I}+\boldsymbol{H}]\cdot(\boldsymbol{u}_{Nr}-\tilde{\boldsymbol{\Phi}}+\boldsymbol{H}\boldsymbol{\Phi})\end{aligned}$$

where $\boldsymbol{w}_i^\top := \boldsymbol{c}^\top[\boldsymbol{I}-\boldsymbol{J}_i] \in \mathbb{R}^{1\times 2}$ is the row-vector of trigonometric polynomials, while $\boldsymbol{H} = \boldsymbol{H}(\boldsymbol{\beta}, \tilde{\boldsymbol{L}}_h, \tilde{\boldsymbol{L}})$ is the matrix introduced in (33). By writing $\beta_i = \beta_{ir} - \tilde{\beta}_i$ and recalling that $\dot{\beta}_{ir} = \boldsymbol{c}^\top[\boldsymbol{I}-\boldsymbol{J}_i(\beta_{ir})]\prod_{j=i}^{N}\boldsymbol{J}_j^{-1}(\beta_{jr})\boldsymbol{u}_{Nr}$ one can observe that under uncertainty conditions

$$\dot{\tilde{\beta}}_i = f_i(\tilde{\boldsymbol{\beta}}_i^N, \boldsymbol{\beta}_r, \boldsymbol{u}_{Nr}) + g_i(\tilde{\boldsymbol{\beta}}_i^N, \boldsymbol{\beta}_r, \tilde{\boldsymbol{\Phi}}) + \nu_i(\tilde{\boldsymbol{\beta}}, \boldsymbol{\beta}_r, \boldsymbol{u}_{Nr}, \tilde{\boldsymbol{\Phi}}), \tag{43}$$

where $f_i(\tilde{\boldsymbol{\beta}}_i^N, \boldsymbol{\beta}_r, \boldsymbol{u}_{Nr})$ and $g_i(\tilde{\boldsymbol{\beta}}_i^N, \boldsymbol{\beta}_r, \tilde{\boldsymbol{\Phi}})$ exactly correspond to the terms from nominal dynamics (24), see [16], while

$$\nu_i(\tilde{\boldsymbol{\beta}}, \boldsymbol{\beta}_r, \boldsymbol{u}_{Nr}, \tilde{\boldsymbol{\Phi}}) = -\boldsymbol{w}_i^\top\boldsymbol{P}_i(\boldsymbol{\beta}_r-\tilde{\boldsymbol{\beta}}, \tilde{\boldsymbol{L}}_h, \tilde{\boldsymbol{L}})(\boldsymbol{u}_{Nr}-\tilde{\boldsymbol{\Phi}}) \tag{44}$$

is the perturbing term depending on $\tilde{\boldsymbol{\Phi}}(t)$ and matrix

$$\boldsymbol{P}_i(\cdot) = \prod_{j=i}^{N}\boldsymbol{J}_j^{-1}(\beta_{jr}-\tilde{\beta}_j)\boldsymbol{H}(\cdot)[2\boldsymbol{I}+\boldsymbol{H}(\cdot)]. \tag{45}$$

According to (36), and recalling the upper bound m_j of the norm $\|\boldsymbol{J}_j^{-1}\|$ (see Section V-A) one may assess

$$\|\boldsymbol{P}_i\| \leq \bar{m}_i\bar{H}(\tilde{\boldsymbol{L}}_h, \tilde{\boldsymbol{L}})[2+\bar{H}(\tilde{\boldsymbol{L}}_h, \tilde{\boldsymbol{L}})] =: \bar{P}_i(\tilde{\boldsymbol{L}}_h, \tilde{\boldsymbol{L}}), \tag{46}$$

where $\bar{m}_i = \prod_{j=i}^{N} m_j$, while $\bar{P}_i : \mathbb{R}^N \times \mathbb{R}^N \to \mathbb{R}_{\geq 0}$ is a function continuous near zero, and $\bar{P}_i(\tilde{\boldsymbol{L}}_h \to \boldsymbol{0}, \tilde{\boldsymbol{L}} \to \boldsymbol{0}) \to 0$.

Under parametric uncertainty the guidance-error $\boldsymbol{e}_N(t)$ is only ultimately bounded. Thus, in this case generally $\tilde{\boldsymbol{\Phi}} \neq \boldsymbol{0}$, and one must keep considering the non-zero term $g_i(\tilde{\boldsymbol{\beta}}_i^N, \boldsymbol{\beta}_r, \tilde{\boldsymbol{\Phi}})$ in (43). Since $\boldsymbol{\beta}_r(t)$ and $\boldsymbol{u}_{Nr}(t)$ are the explicit functions of time only, one may write (43) for $i = 1, \ldots, N$ as

$$\dot{\tilde{\boldsymbol{\beta}}} = \boldsymbol{f}(\tilde{\boldsymbol{\beta}}, t) + \boldsymbol{p}(\tilde{\boldsymbol{\beta}}, t) = \begin{bmatrix} f_1(\tilde{\boldsymbol{\beta}}, t) + p_1(\tilde{\boldsymbol{\beta}}, t) \\ \vdots \\ f_N(\tilde{\boldsymbol{\beta}}, t) + p_N(\tilde{\boldsymbol{\beta}}, t)\end{bmatrix}, \tag{47}$$

where the resultant ith perturbation term

$$p_i(\tilde{\boldsymbol{\beta}}, t) = g_i(\tilde{\boldsymbol{\beta}}, t, \tilde{\boldsymbol{\Phi}}(t)) + \nu_i(\tilde{\boldsymbol{\beta}}, t, \tilde{\boldsymbol{\Phi}}(t)) \tag{48}$$

with

$$g_i(\tilde{\boldsymbol{\beta}}, t, \tilde{\boldsymbol{\Phi}}(t)) = \boldsymbol{w}_i^\top\prod_{j=i}^{N}\boldsymbol{J}_j^{-1}(\beta_{jr}(t)-\tilde{\beta}_j)\tilde{\boldsymbol{\Phi}}(t) \tag{49}$$

and $\nu_i(\tilde{\boldsymbol{\beta}}, t, \tilde{\boldsymbol{\Phi}}(t))$ determined by (44) depends on the nominal outer-loop control difference $\tilde{\boldsymbol{\Phi}}(t)$. Since in general $\boldsymbol{p}(\boldsymbol{0}, t) \not\equiv \boldsymbol{0}$, we cannot treat $\tilde{\boldsymbol{\beta}} = \boldsymbol{0}$ as an equilibrium of perturbed dynamics (47). However, we can still show the ultimate boundedness of $\tilde{\boldsymbol{\beta}}(t)$. According to (48) and by utilizing (44), (49), (46), and property P1 one can show that

$$\begin{aligned}\left|p_i(\tilde{\boldsymbol{\beta}}, t)\right| &\leq \left|g_i(\tilde{\boldsymbol{\beta}}, t, \tilde{\boldsymbol{\Phi}}(t))\right| + \left|\nu_i(\tilde{\boldsymbol{\beta}}, t, \tilde{\boldsymbol{\Phi}}(t))\right|\\ &\leq \bar{w}_i\bar{m}_i\|\tilde{\boldsymbol{\Phi}}\| + \bar{w}_i\bar{\phi}\bar{P}_i(\tilde{\boldsymbol{L}}_h, \tilde{\boldsymbol{L}}) =: \bar{p}_i\left(\tilde{\boldsymbol{\Phi}}, \tilde{\boldsymbol{L}}_h, \tilde{\boldsymbol{L}}\right)\end{aligned} \tag{50}$$

where $\bar{m}_i = \prod_{j=i}^{N} m_j$, while $\bar{w}_i > 0$ is a finite upper bound of $\|\boldsymbol{w}_i\|$. Upon definition (22), condition C3, and property P1 holds $\|\tilde{\boldsymbol{\Phi}}\| \leq (\bar{u}_r + \bar{\phi}) < \infty$, thus all the terms on the right-hand side of (50) are bounded ensuring $\bar{p}_i(\cdot) < \infty$. It is clear that $\bar{p}_i(\boldsymbol{0}, \boldsymbol{0}, \boldsymbol{0}) = 0$. Moreover, $\tilde{\boldsymbol{\Phi}}(t) \overset{(22)}{=} \tilde{\boldsymbol{\Phi}}(\boldsymbol{e}_N(t), t)$ and $\tilde{\boldsymbol{\Phi}}(\boldsymbol{0}_{2\mu\pi}, t) \equiv \boldsymbol{0}$ upon property P2. Thus, $\bar{p}_i(\tilde{\boldsymbol{\Phi}}(t), \boldsymbol{0}, \boldsymbol{0}) \to 0$ as $t \to T$, $T \in (0, \infty)$, due to asymptotic convergence $\boldsymbol{e}_N(t) \to \boldsymbol{0}_{2\mu\pi}$ in the nominal case. As a consequence of (50),

$$\forall\, t \geq 0 \;\; \|\boldsymbol{p}(\tilde{\boldsymbol{\beta}}, t)\| \leq \sqrt{\bar{p}_1^2 + \ldots + \bar{p}_N^2} =: \bar{p}(\tilde{\boldsymbol{\Phi}}, \tilde{\boldsymbol{L}}_h, \tilde{\boldsymbol{L}})$$

and the upper bound $\bar{p}(\boldsymbol{0}, \boldsymbol{0}, \boldsymbol{0}) = 0$. Since $\tilde{\boldsymbol{\beta}} = \boldsymbol{0}$ is the locally (uniformly in time) exponentially stable equilibrium of nominal zero-dynamics $\dot{\tilde{\boldsymbol{\beta}}} = \boldsymbol{f}(\tilde{\boldsymbol{\beta}}, t)$ (approximated by (27)), one can use Lemma 9.3 from [11] to state what follows.

Corollary 2: For sufficiently small $\bar{p}(\tilde{\boldsymbol{\Phi}}, \tilde{\boldsymbol{L}}_h, \tilde{\boldsymbol{L}})$, corresponding to sufficiently small $\|\tilde{\boldsymbol{\Phi}}\|$, $\left|\tilde{L}_{hi}\right|$, and $\left|\tilde{L}_i\right|$ for $i = 1, \ldots, N$, and for sufficiently small $\|\tilde{\boldsymbol{\beta}}(0)\|$ the solution of perturbed dynamics (47) is ultimately bounded (uniformly in time) satisfying

$$\|\tilde{\boldsymbol{\beta}}(t)\| \leq \xi_\beta\left(\|\tilde{\boldsymbol{\beta}}(0)\|, t\right) \qquad \text{for } t \in [0, T_\beta), \tag{51}$$

$$\|\tilde{\boldsymbol{\beta}}(t)\| \leq \kappa_\beta\left(\bar{p}(\tilde{\boldsymbol{\Phi}}, \tilde{\boldsymbol{L}}_h, \tilde{\boldsymbol{L}})\right) \qquad \text{for } t \in [T_\beta, \infty), \tag{52}$$

where $T_\beta > 0$ denotes a finite time instant, ξ_β is a function of class $\mathcal{KL}$, while κ_β is a function of class $\mathcal{K}$.

Remark 4: If a particular form of control function $\boldsymbol{\Phi}(\boldsymbol{e}_N, t)$ is considered, it may be possible to formulate additional conclusions on a magnitude of $\|\tilde{\boldsymbol{\Phi}}\|$ in (50). Namely, if for the particular $\boldsymbol{\Phi}(\boldsymbol{e}_N, t)$ the norm of $\tilde{\boldsymbol{\Phi}}(t) \overset{(22)}{=} \boldsymbol{u}_{Nr}(t) - \boldsymbol{\Phi}(\boldsymbol{e}_N, t)$ can be upper bounded by some $\mathcal{K}$-class function $\kappa_\phi(\|\boldsymbol{e}_N\|)$, then one can utilize result (40) to state that

$$\|\tilde{\boldsymbol{\Phi}}\| \leq \kappa_\phi(\|\boldsymbol{e}_N\|) \leq \kappa_\phi(\kappa_e(\bar{d}(\tilde{\boldsymbol{L}}_h, \tilde{\boldsymbol{L}}))) =: \tilde{\phi}(\tilde{\boldsymbol{L}}_h, \tilde{\boldsymbol{L}}) \tag{53}$$

where $\tilde{\phi} : \mathbb{R}^N \times \mathbb{R}^N \to \mathbb{R}_{\geq 0}$ is a function continuous near zero, and $\tilde{\phi}(\tilde{\boldsymbol{L}}_h \to 0, \tilde{\boldsymbol{L}} \to 0) \to 0$. As a consequence, $\bar{p}_i = \bar{p}_i(\tilde{\boldsymbol{L}}_h, \tilde{\boldsymbol{L}})$ and $\bar{p} = \bar{p}(\tilde{\boldsymbol{L}}_h, \tilde{\boldsymbol{L}})$ become the continuous near zero functions of parameter errors, and $\bar{p}(\tilde{\boldsymbol{L}}_h \to 0, \tilde{\boldsymbol{L}} \to 0) \to 0$.

VI. Experimental verification of the method

Control performance has been verified with a three-trailer nS3T vehicle with adjustable hitching offsets and constant trailer lengths $L_1 = L_2 = L_3 = 0.229\,\text{m}$ (see Fig. 3). The vehicle tractor was equipped with two brushless DC motors (50W, Maxon EC 45-flat with gearboxes 47:1) closed with the PI-type speed control loops used for the two actuated wheels. Joint angles were measured by absolute 14-bit encoders (Hengstler AD36). Robust estimation of the last trailer posture $\boldsymbol{q}_N$ was possible thanks to the fusion of a software predictor estimate (computed with frequency of $100\,\text{Hz}$) with

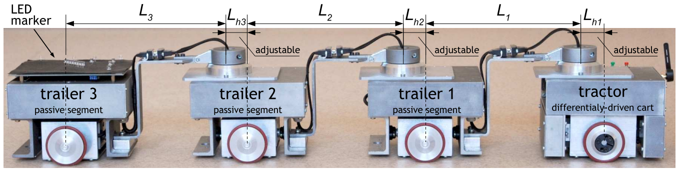

Fig. 3. The laboratory-scale articulated vehicle used in the experiments.

TABLE I
CONDITIONS PRESCRIBED FOR THE PARTICULAR EXPERIMENTS

Exp.	Reference trajectory	Offsets [m]	Conditions
EA	$x_{3r}(t) = 0.4\sin(0.1t)$ $y_{3r}(t) = 0.3\sin(0.15t)$	$L_{h1} = +0.048$ $L_{h2} = +0.048$ $L_{h3} = +0.032$	nominal backward tracking
EB	$x_{3r}(t) = 0.4\cos(0.1t)$ $y_{3r}(t) = 0.3\sin(0.1t)$	$L_{h1} = +0.048$ $L_{h2} = +0.048$ $L_{h3} = -0.008$	backward tracking violating A2
EC	$x_{3r}(t) = 0.4\cos(0.05t)$ $y_{3r}(t) = 0.3\sin(0.05t)$	$L_{h1} = -0.008$ $L_{h2} = -0.008$ $L_{h3} = -0.008$	uncertain forward tracking

a vision estimate obtained from an external calibrated vision system (PC + camera uEye UI-1240SE-C with resolution 1280x1024 and sampling 25Hz) employed for recognition of a LED marker mounted on a top of the guidance segment (see Fig. 3). The cascade-like controller was implemented on the on-board floating-point DSP processor (TMS320F28335) with sampling frequency of $100\,\mathrm{Hz}$. During experiments, the so-called *Velocity Scaling Block*, see [15], [17], was employed in series with the proposed controller to take into account control-input limitations resulting from a finite maximal admissible velocity $\omega_m > 0$ of a tractor wheel (i.e., vector (20) were on-line postprocessed using the prescribed value of $\omega_m = 10\,\mathrm{rad/s}$ leading to the scaled control $\boldsymbol{u}_{0s} = [\omega_{0s}\ v_{0s}]^\top$ applied to the tractor). For more details on the experimental testbed see [17].

For control purposes, the outer-loop controller $\boldsymbol{\Phi}(\boldsymbol{e}_N, t) = \boldsymbol{\Phi}^{\mathrm{S}}(\boldsymbol{e}_N, t)$ proposed in [6] has been applied, where

$$\boldsymbol{\Phi}^{\mathrm{S}}(\boldsymbol{e}_N, t) \triangleq \begin{bmatrix} \omega_{Nr} + k_0 v_{Nr}\tilde{e}_3 \mathrm{s}e_\theta / e_\theta + k_1(\boldsymbol{u}_{Nr})e_\theta \\ v_{Nr}\mathrm{c}e_\theta + k_2(\boldsymbol{u}_{Nr})\tilde{e}_2 \end{bmatrix},$$

with $\tilde{e}_2 = e_x \mathrm{c}\theta_N + e_y \mathrm{s}\theta_N$, $\tilde{e}_3 = -e_x \mathrm{s}\theta_N + e_y \mathrm{c}\theta_N$, $k_1(\boldsymbol{u}_{Nr}) = k_2(\boldsymbol{u}_{Nr}) \triangleq 2\xi\sqrt{\omega_{Nr}^2 + k_0 v_{Nr}^2}$, and parameters $k_0 > 0$, $\xi > 0$. Note that $\boldsymbol{\Phi}^{\mathrm{S}}$ satisfies property P3 globally for $\mu = 0$, see [6].

Results of three experiments (EA, EB, and EC) have been presented in Fig. 4. Table I explains conditions prescribed for the particular tests. In all the experiments $k_0 = 90$, $\xi = 1.0$.

Analyzing the plots in Fig. 4 worth to emphasize smooth motion of the guidance segment and agile maneuvers performed by the vehicle during transient stages of all the experiments. Results of experiment EA illustrate control performance obtained under almost nominal conditions (i.e., for negligible parametric uncertainty) preserving assumption A2.

Results of experiment EB illustrate relative robustness of the closed-loop system to violation of assumption A2. In this case, the approximated matrix (29) was used for $i = 3$ employing $\hat{L}_{h3} = +0.016\,\mathrm{m}$, which implies substantial parametric uncertainty corresponding to $\rho_{h3} = -2.0$ (uncertainty concerns both the value and the sign of L_{h3}). In experiment EB robustness of the closed-loop system was intensionally utilized to overcome limitations imposed by assumption A2 while simultaneously preserving acceptable control performance.

Results of experiment EC show, on one hand, how the small absolute values of hitching offsets increase noise sensitivity of the closed-loop system (see increased oscillations of ω_{0s}). On the other hand, they illustrate how one may intentionally utilize robustness property to attenuate the resultant noise sensitivity and obtain acceptable tracking performance. It was possible by using approximated matrices (29) in the inner loop with artificially increased absolute values of $\hat{L}_{hi} = -0.016\,\mathrm{m}$ for $i = 1, 2, 3$ which correspond to uncertainty coefficients $\rho_{h1} = \rho_{h2} = \rho_{h3} = +2.0$. This approach turned out to be effective, however, only if the vehicle motion was initialized in a sufficiently small neighborhood of the reference trajectory.

VII. CONCLUDING REMARKS

The cascade-like control framework presented in the paper provides a highly scalable and modular solution to the trajectory tracking control problem for nSNT kinematics, generalizing in various directions the original solution presented for a particular case in [5].

Worth to emphasize relative application simplicity of the method irrespectively of a number of trailers present in a vehicle (scalability), and its modular character where the outer-loop feedback controller can be flexibly selected/replaced according to different design criteria like robustness, simplicity of tuning and implementation, transient and steady performance, or simply some preferences of a designer. Limitations of the method mainly come from assumptions A1 and A2. It seems that relaxation of assumption A1 could be possible by a combination of the presented solution and the one proposed in [7], however this issue requires further investigations. Restriction A2 seems not very limiting since the sign-homogeneous hitching is characteristic for most practical constructions of the nSNT vehicles, especially in the area of robotics.

REFERENCES

[1] C. Altafini. Some properties of the general n-trailer. *Int. J. Control*, 74(4):409–424, 2001.

[2] C. Altafini. Path following with reduced off-tracking for multibody wheeled vehicles. *IEEE Trans. Cont. Syst. Techn.*, 11(4):598–605, 2003.

[3] P. Bolzern, R. M. DeSantis, and A. Locatelli. An input-output linearization approach to the control of an n-body articulated vehicle. *ASME J. Dyn. Syst., Meas., and Control*, 123:309–316, 2001.

[4] P. Bolzern, R. M. DeSantis, A. Locatelli, and D. Masciocchi. Path-tracking for articulated vehicles with off-axle hitching. *IEEE Trans. Control Syst. Technol.*, 6(4):515–523, 1998.

[5] W. Chung, M. Park, K. Yoo, J. I. Roh, and J. Choi. Backward-motion control of a mobile robot with n passive off-hooked trailers. *J. Mechanical Science and Technology*, 25(11):2895–2905, 2011.

[6] C. Canudas de Wit, H. Khennouf, C. Samson, and O.J. Sørdalen. Nonlinear control design for mobile robots. In Y.F. Zheng, editor, *Recent Trends in Mobile Robots*, volume 11, chapter 5, pages 121–156. World Scientific, Singapore, 1993.

[7] M. Michałek. Tracking control strategy for the standard N-trailer mobile robot – a geometrically motivated approach. In K. Kozłowski, editor, *Robot Motion and Control 2011*, volume 422 of *Lecture Notes in Control and Information Sciences*, pages 39–51. Springer, 2012.

[8] M. Michałek. Non-minimum-phase property of N-trailer kinematics resulting from off-axle interconnections. *Int. Journal of Control*, 86(4):740–758, 2013.

[9] Z. Huofeng and M. Baoli. Path following control of tractor-trailers with off-axle hitching. In *Chinese Control Conference CCC 2007*, pages 283–286, Hunan, China, 2007.

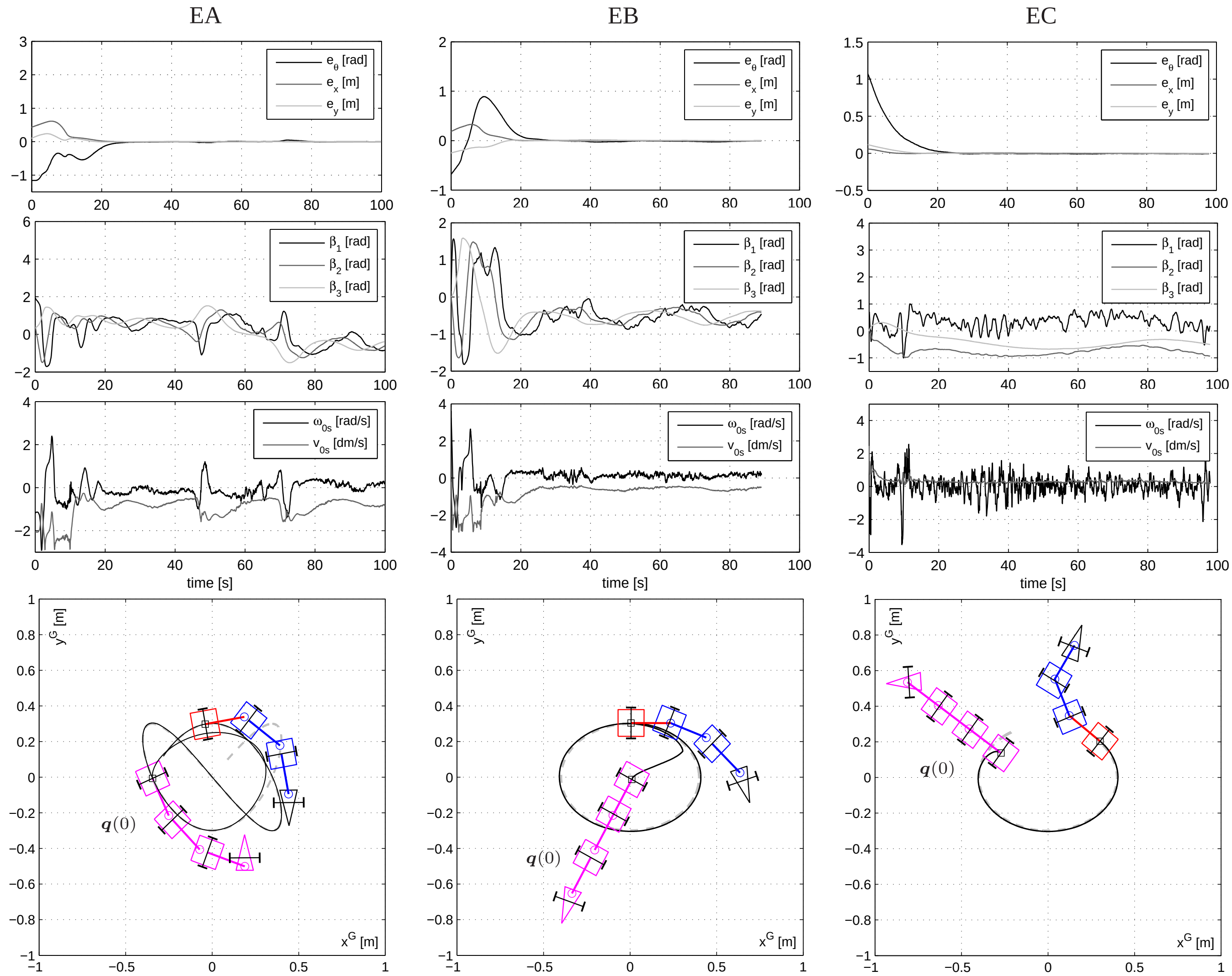

Fig. 4. Results of three experimental tests: for backward motion under nominal conditions (EA), for backward motion with uncertainty in L_{h3} offset (EB), and for forward motion with substantial uncertainty in all the hitching offsets (EC); initial vehicle configuration $\boldsymbol{q}(0)$ has been highlighted in magenta.

[10] F. Jean. The car with N trailers: characterisation of the singular configurations. *Control, Opt. Calc. Variations*, 1:241–266, 1996.

[11] H. K. Khalil. *Nonlinear systems. 3-Ed.* Prentice-Hall, New Jersey, 2002.

[12] J. P. Laumond. Controllability of a multibody mobile robot. *IEEE Trans. Robot. Autom.*, 9(6):755–763, 1993.

[13] S.-J. Li and W. Respondek. Flat outputs of two-input driftless control systems. *ESAIM: Control, Optim. Calc. Variations*, 18:774–798, 2012.

[14] D. A. Lizarraga, P. Morin, and C. Samson. Chained form approximation of a driftless system. Application to the exponential stabilization of the general N-trailer system. *Int. J. Control*, 74(16):1612–1629, 2001.

[15] M. M. Michałek. A highly scalable path-following controller for N-trailers with off-axle hitching. *Control Eng. Practice*, 29:61–73, 2014.

[16] M. M. Michałek. Modular tracking controller for N-trailers with non-zero hitching offsets. In *2015 American Control Conference*, pages 5371–5376, Chicago, USA, 2015.

[17] M. M. Michałek, M. Kiełczewski, and T. Jedwabny. Cascaded VFO control for non-standard N-trailer robots. *J Intell Robot Syst*, 77(3-4):415–432, 2015.

[18] J. Morales, J. L. Martinez, A. Mandow, and A. J. Gracia-Cerezo. Steering the last trailer as a virtual tractor for reversing vehicles with passive on- and off-axle hitches. *IEEE Trans. Industrial Electronics*, 60(12):5729–5736, 2013.

[19] P. Morin and C. Samson. Transverse function control of a class of non-invariant driftless systems. Application to vehicles with trailers. In *47th IEEE Conf. Dec. Control*, pages 4312–4319, Cancun, Mexico, 2008.

[20] P. Morin and C. Samson. Motion control of wheeled mobile robots. In *Springer Handbook of Robotics*, pages 799–826. Springer, Berlin, 2008.

[21] G. Oriolo and M. Vendittelli. A framework for the stabilization of general nonholonomic systems with an application to the plate-ball mechanism. *IEEE Trans. Robot.*, 21(2):162–175, 2005.

[22] D. Pazderski, D. Waśkowicz, and K. Kozłowski. Motion control of vehicles with trailers using transverse function approach. Controller properties analysis. *J Intell Robot Syst*, 77(3-4):457–479, 2015.

[23] O. J. Sørdalen. Conversion of the kinematics of a car with n trailers into a chained form. In *Proc. IEEE Int. Conf. on Robotics and Automation*, pages 382–387, Atlanta, USA, 1993.

[24] O. J. Sørdalen and K. Y. Wichlund. Exponential stabilization of a car with n trailers. In *Proceedings of the 32th Conference on Decision and Control*, pages 978–983, San Antonio, USA, 1993.

[25] H. H. Rosenbrook. The stability of linear time-dependent control systems. *J. Electronics and Control*, 15(1):73–80, 1963.

[26] P. Rouchon, M. Fliess, J. Levine, and P. Martin. Flatness, motion planning and trailer systems. In *Proceedings of the 32nd Conference on Decision and Control*, pages 2700–2705, San Antonio, Texas, 1993.

[27] C. Samson. Control of chained systems. Application to path following and time-varying point-stabilization of mobile robots. *IEEE Trans. Autom. Control*, 40(1):64–77, 1995.

[28] K. Yoo and W. Chung. Pushing motion control of n passive off-hooked trailers by a car-like mobile robot. In *2010 IEEE int. Conf. Robotics and Automation*, pages 4928–4933, Anchorage, USA, 2010.

[29] J. J. Zhu. A note on extension of the eigenvalue concept. *IEEE Control Systems*, 13(6):68–70, 1993.